Supplementary Methods

MRI acquisition. Using a 3.0 Tesla scanner (Philips Medical Systems, Eindhoven, the Netherlands), the following brain images were obtained: a) dual-echo turbo spin echo (TSE) (repetition time [TR]/echo time [TE]=2599/16,80 ms, echo train length=6, 44 contiguous 3-mm-thick axial slices with a matrix size=256×256, FOV=240 mm2); b) 3D T1-weighted fast field echo (TR/TE=25/4.6 ms; flip angle=30°; matrix size=256×256; FOV=230×230 mm2; 220 contiguous, axial slices with voxel size=0.89×0.89×0.8 mm; and c) pulsed-gradient SE echo-planar (EP) (TE/TR=58/8775 ms, acquisition matrix size=112×88, FOV=240×231 mm2, 55 contiguous, 2.3 mm thick axial slices) with SENSE (acceleration factor=2) and diffusion gradients applied in 35 non-collinear directions. Two optimized b factors were used for acquiring diffusion weighted images (b1=0, b2=900 s/mm^2). For all scans, the slices were positioned to run parallel to a line that joins the most infero-anterior and infero-posterior margins of the corpus callosum.

Lesion distribution. 2D histograms were produced for each patient having the ratio of the number of transected fibers per fiber bundle on the y axis and one of the following metrics on the x axis: average fractional anisotropy (FA), average length of fibers and average number of fibers. Histograms were averaged for the whole group of multiple sclerosis (MS) patients and for each disease clinical phenotype. Moreover, the transection ratio was calculated for the 116 nodes of the network and averaged within macro-areas; the following macro-areas were considered based on anatomical criteria: frontal, temporal, limbic, occipital, parietal, deep GM nuclei and cerebellar (supplementary Table 1). Using a one-way ANOVA model, comparisons between clinical phenotypes were assessed.

Cross validation. The dataset was subsampled 100 times, extracting 75 patients and 35 healthy controls. Each time, subject selection was accomplished using a pseudo random generator. Any constraint was used to keep the proportion of MS clinical phenotypes constant, although in all cases there was a good approximation of the original distribution. The same statistical tests were applied as for the original data set, to assess between-group comparisons of global network metrics and

correlations with clinical scores. The percentage of significant results was then calculated over the 100 subsamples tested, limiting cross-validation to global metrics.

Supplementary Results

Distribution of transected fiber bundles: 2D histograms. Supplementary Fig. 1 shows 2D histograms of the dependence of transection on FA (A), fiber length (B) and number of fibers per fiber bundle (C). The majority of transected fiber bundles are in histogram bins within the following ranges: FA=0.4-0.45, length=150-165 mm and number of fibers=5-30; in these bins, an a posteriori statistical analysis (ANOVA model) found significant differences between relapsing remitting (RR) MS and both benign MS and secondary progressive (SP) MS patients and no differences between SPMS and benign MS patients (Supplementary Table 2). Although the degree of transection ranged from 0 to 1, the vast majority of fiber tracts showed either no disconnection or complete disconnection.

Transection affecting nodes. Moving from RRMS to benign and SPMS, transection ratio increased in all nodes in a similar way. The most affected nodes, common to all MS clinical phenotypes, were the superior occipital gyri, paracentral lobules, right (R) superior parietal lobule, left (L) caudate nucleus, L and R thalamus, R middle temporal gyrus and L cuneus (Supplementary Fig. 2). The average transection ratio in nodes classified according to macro-area membership was highest for deep gray matter nuclei, high for the occipital, parietal and temporal regions, medium for the frontal regions and low for the limbic system and cerebellum. This behavior was similar for all MS clinical phenotypes. Statistical analysis revealed that the average nodal transection ratio in each macro-area was always significantly different between RRMS and SPMS patients and for the majority of macro-areas between RRMS and benign MS patients. No difference was found between SPMS and benign MS patients, except for the cerebellum (Supplementary Table 3).

Cross validation. The percentage of significant results over the 100 subsamples tested, are the followings for the between group comparisons:

Mean Strength: RRvsHC 100%, SPvsRR 68%, BvsRR 33%, SPvsB 3%
Transitivity: RRvsHC 100%, SPvsRR 66%, BvsRR 33%, SPvsB 3%,
Global efficiency: RRvsHC 100%, SPvsRR 68%, BvsRR 32%, SPvsB 3%,
Assortativity: RRvsHC 100%, SPvsRR 6%, BvsRR 3%, SPvsB 0%,
Characteristic path length: RRvsHC 94%, SPvsRR 69%, BvsRR 20%, SPvsB 9%,

These are the results after modelling of disconnection:

Mean Strength: RRvsHC 100%, SPvsRR 84%, BvsRR 39%, SPvsB 6%,
Transitivity: RRvsHC 100%, SPvsRR 85%, BvsRR 36%, SPvsB 3%,
Global efficiency: RRvsHC 100%, SPvsRR 81%, BvsRR 34%, SPvsB 5%,
Assortativity: RRvsHC 0%, SPvsRR 52%, BvsRR 11%, SPvsB 7%,
Characteristic path length: RRvsHC 100%, SPvsRR 81%, BvsRR 20%, SPvsB 14%,

These results suggest that reducing the sample size to one third implies that the only comparison that is still robustly found is between RRMS and HC. The modelling of disconnection slightly improved the percentage of significant results. Assortativity was confirmed as the test that changed behaviour after disconnection.

It was confirmed that correlations with GM atrophy are strong. Disease duration was often a significant factor (on average 70% of times found), whereas EDSS, PASAT and WM atrophy were significant in less than 50 percent of the subsamples. The modelling of disconnection did not change these results.

Supplementary Table 1. Brain nodes of the network based on the AAL atlas. Odd label numbers refer to the left hemisphere, and the even numbers to the right hemisphere. The column indicating the membership of macro-areas was assigned using anatomical criteria.

AAL label number	AAL label name	Anatomical region	Macro-area	AAL label number	AAL label name	Anatomical region	Macro-area	AAL label number	Aal Label Name	Anatomical region	Macro-area
1; 2	Precentral	Precentral gyrus	Frontal	43; 44	Calcarine	Calcarine sulcus	Occ	85; 86	Temporal_Mid	Middle temporal gyrus	Temp
3; 4	Frontal_Sup	Superior frontal gyrus	Frontal	45; 46	Cuneus	Cuneus	Occ	87; 88	Temporal_Pole_Mid	Middle temporal pole	Temp
5; 6	Frontal_Sup_Orb	Superior frontal gyrus, orbital part	Frontal	47; 48	Lingual	Lingual gyrus	Occ	89; 90	Temporal_Inf	Inferior temporal gyrus	Temp
7; 8	Frontal_Mid	Middle frontal gyrus	Frontal	49; 50	Occipital_Sup	Superior occipital gyrus	Occ	91; 92	Cerebelum_Crus1	Crus i of cerebellar hemisphere	Cereb
9; 10	Frontal_Mid_Orb	Middle frontal gyrus, orbital part	Frontal	51; 52	Occipital_Mid	Middle occipital gyrus	Occ	93; 94	Cerebelum_Crus2	Crus ii of cerebellar hemisphere	Cereb
11; 12	Frontal_Inf_Oper	Inferior frontal gyrus, pars opercularis	Frontal	53; 54	Occipital_Inf	Inferior occipital cortex	Occ	95; 96	Cerebelum_3	Lobule iii of cerebellar hemisphere	Cereb
13; 14	Frontal_Inf_Tri	Inferior frontal gyrus, pars triangularis	Frontal	55; 56	Fusiform	Fusiform gyrus	Occ	97; 98	Cerebelum_4_5	Lobule iv, v of cerebellar hemisphere	Cereb
15; 16	Frontal_Inf_Orb	Inferior frontal gyrus, pars orbitalis	Frontal	57; 58	Postcentral	Postcentral gyrus	Parietal	99; 100	Cerebelum_6	Lobule vi of cerebellar hemisphere	Cereb
17; 18	Rolandic_Oper	Rolandic operculum	Frontal	59; 60	Parietal_Sup	Superior parietal lobule	Parietal	101; 102	Cerebelum_7b	Lobule viib of cerebellar	Cereb

										hemisphere	
19; 20	Supp_Motor_Area	Supplementary motor area	Frontal	61; 62	Parietal_Inf	Inferior parietal lobule	Parietal	103; 104	Cerebelum_8	Lobule viii of cerebellar hemisphere	Cereb
21; 22	Olfactory	Olfactory cortex	Frontal	63; 64	Supramarginal	*Supramarginal gyrus*	Parietal	105; 106	Cerebelum_9	Lobule ix of cerebellar hemisphere	Cereb
23; 24	Frontal_Sup_Medial	Medial frontal gyrus	Frontal	65; 66	Angular	Angular gyrus	Parietal	107; 108	Cerebelum_10	Lobule x of cerebellar hemisphere	Cereb
25; 26	Frontal_Mid_Orb	Medial orbitofrontal cortex	Frontal	67; 68	Precuneus	Precuneus	Parietal	109	Vermis_1_2	Lobule i, ii of vermis	Cereb
27; 28	Rectus	Gyrus rectus	Frontal	69; 70	Paracentral_Lobule	Paracentral lobule	Parietal	110	Vermis_3	Lobule iii of vermis	Cereb
29; 30	Insula	Insula	Temp	71; 72	Caudate	Caudate nucleus	DGM	111	Vermis_4_5	Lobule iv, v of vermis	Cereb
31; 32	Cingulum_Ant	Anterior cingulate gyrus	Limbic	73; 74	Putamen	Putamen	DGM	112	Vermis_6	Lobule vi of vermis	Cereb
33; 34	Cingulum_Mid	Midcingulate area	Limbic	75; 76	Pallidum	Globus pallidus	DGM	113	Vermis_7	Lobule vii of vermis	Cereb
35; 36	Cingulum_Post	Posterior cingulate gyrus	Limbic	77; 78	Thalamus	Thalamus	DGM	114	Vermis_8	Lobule viii of vermis	Cereb
37; 38	Hippocampus	Hippocampus	Limbic	79; 80	Heschl	Transverse temporal gyrus	Temp	115	Vermis_9	Lobule ix of vermis	Cereb
39; 40	Parahippocampal	Parahippocampal gyrus	Limbic	81; 82	Temporal_Sup	Superior temporal gyrus	Temp	116	Vermis_10	Lobule x of vermis	Cereb
41; 42	Amygdala	Amygdala	Limbic	83; 84	Temporal_Pole_Sup	Superior temporal pole	Temp				

Abbreviations: AAL: Automated Anatomical Labeling; Temp=Temporal; Occ=Occipital; DGM=Deep Grey Matter Nuclei; Cereb=Cerebellar.

Supplementary Table 2. Between-group comparisons of percentage of white matter tracts studied for transection ratios of 0 and 1, and for the metrics reported in column 1. Estimated means and standard errors resulting from the fitting of a one-way ANOVA model are reported for each group.

Tract metric	Transection ratio	RRMS	Benign MS	P value*	SPMS	P value**	P value***
FA=0.4-0.45	0	8.7 (0.5)	5.3 (0.8)	<0.001	4.6 (0.6)	<0.001	n.s.
	1	5.4 (0.5)	8.6 (0.8)	0.003	10.1 (0.7)	<0.001	n.s.
Length=150-165 mm	0	4.3 (0.2)	2.9 (0.4)	0.005	2.5 (0.3)	<0.001	n.s.
	1	2.0 (0.2)	3.3 (0.4)	0.008	4.1 (0.3)	<0.001	n.s.
#Tracts=5-30	0	20.2 (0.6)	16.9 (0.9)	0.005	15.3 (0.7)	<0.001	n.s.
	1	6.6 (0.5)	9.7 (0.8)	0.005	11.4 (0.7)	<0.001	n.s.

P values refer to one-way ANOVA model (post-hoc comparisons with Bonferroni correction applied).

**Benign vs RRMS; **SPMS vs RRMS; ***SPMS vs Benign MS.*

Abbreviations: FA=fractional anisotropy; MS=multiple sclerosis; RR=relapsing-remitting; SP=secondary progressive; n.s.=not significant.

Supplementary Table 3. Between-group comparison of average nodal disconnection ratio in each macro-area. Estimated means and standard errors resulting from the fitting of a one-way ANOVA model are reported for each group.

Macro-area	RRMS	Benign MS	p value*	SPMS	p value**	p value***
Deep gray matter nuclei	0.29 (0.02)	0.44 (0.03)	0.001	0.50 (0.03)	<0.001	n.s.
Occipital	0.26 (0.02)	0.35 (0.03)	0.01	0.39 (0.02)	<0.001	n.s.
Temporal	0.21 (0.02)	0.31 (0.03)	0.001	0.34 (0.02)	<0.001	n.s.
Parietal	0.21 (0.02)	0.30 (0.03)	0.009	0.34 (0.02)	<0.001	n.s.
Frontal	0.16 (0.01)	0.23 (0.02)	0.04	0.29 (0.02)	<0.001	n.s.
Limbic	0.05 (0.01)	0.07 (0.01)	n.s.	0.10 (0.01)	<0.001	n.s.
Cerebellum	0.05 (0.005)	0.06 (0.007)	n.s.	0.09 (0.006)	<0.001	0.05

p-values refer to one-way ANOVA model (post-hoc comparisons with Bonferroni correction applied).

**Benign multiple sclerosis vs RRMS; **SPMS vs RRMS; ***SPMS vs benign MS.*

Abbreviations: RR=relapsing-remitting; SP=secondary progressive; n.s.=not significant.

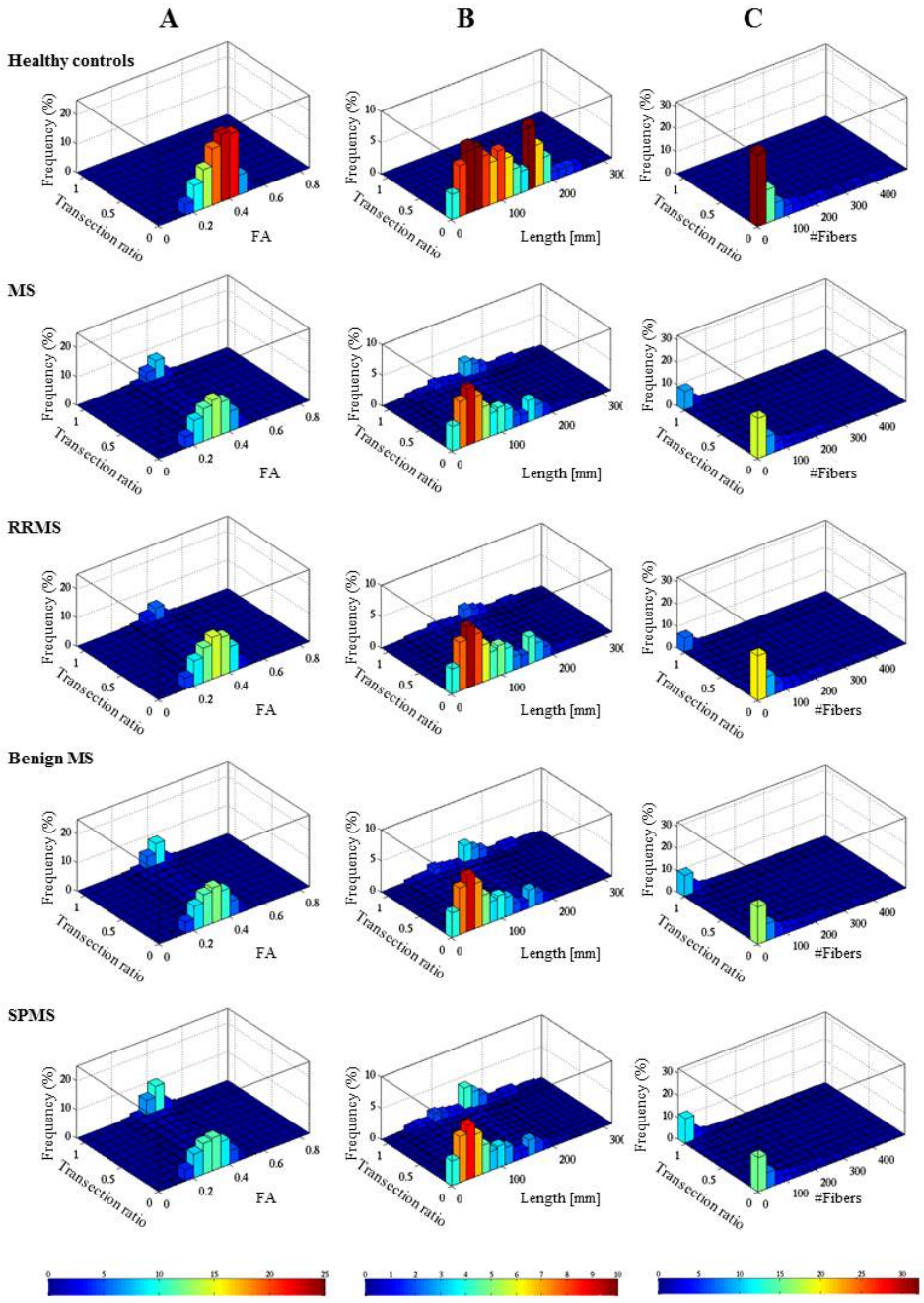

Supplementary Figure 1. **Dependence of transection ratio on white matter fiber bundle properties in the custom atlas.** The figure shows 2D histograms of the dependence of transection on FA (A), fiber length (B) and number of fibers per fiber bundle (C). The first panel of the figure shows the distributions in fiber bundles for healthy controls (HCs). In the subsequent panels, the effect of transection is shown for all MS patients, and separately for relapsing remitting (RR) MS, benign MS and secondary progressive (SP) MS patients.

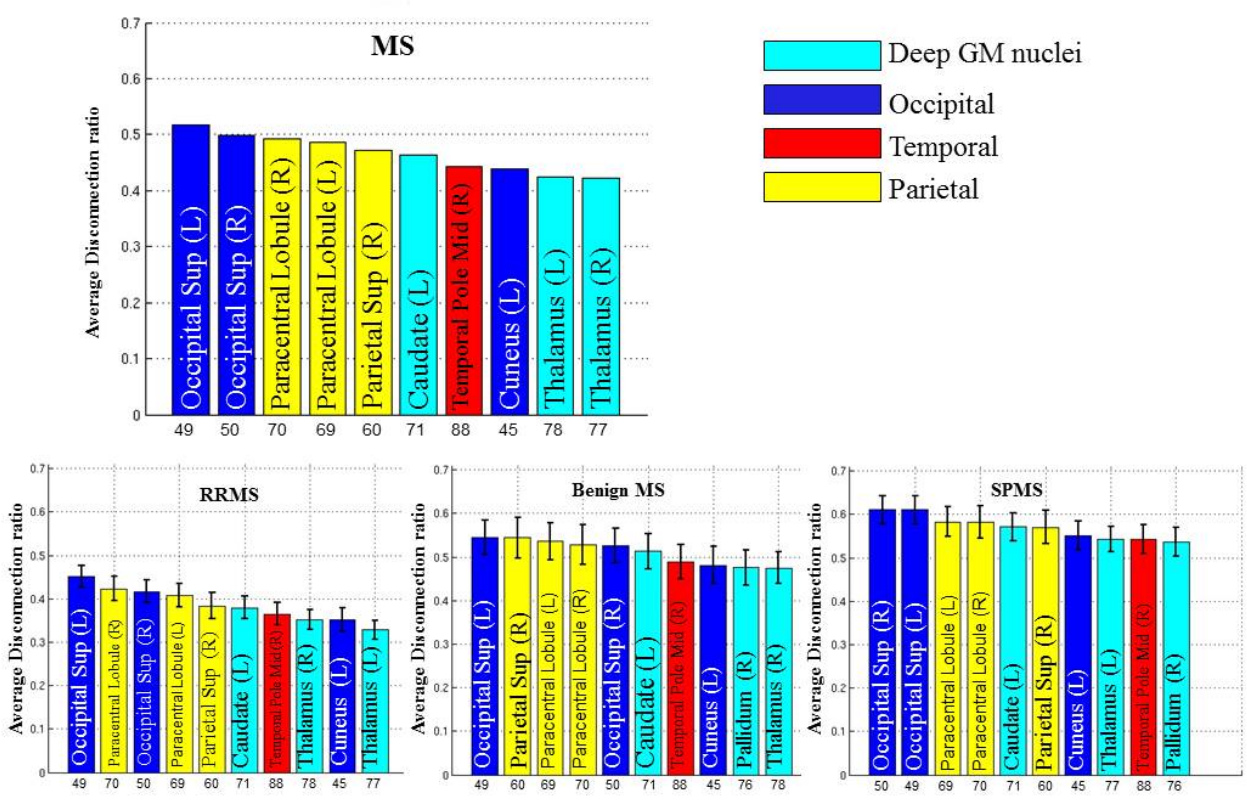

Supplementary Figure 2. First 10 nodes with the highest average transection ratios. Average values and standard errors are reported. Bars are colored according to macro-area membership. Nodes are identified using the AAL labels described in Supplementary Table 1. Abbreviations: RR=relapsing-remitting; SP=secondary progressive; MS=multiple sclerosis.